Research

Chaotic Metasurfaces

Ribaš Anja[1,*]

[1.] University of Maribor, Faculty of Natural Sciences and Mathematics, Department of Physics
* Correspondence: Anja Ribaš: anja.ribas@student.um.si

Citation: Ribaš A. Chaotic Metasurfaces. Proceedings of Socratic Lectures. **2026**, 14, 63-68. https://doi.org/10.55295/PSL.14.2026.III5

Publisher's Note: UL ZF stays neutral about jurisdictional claims in published maps and institutional affiliations.

Abstract:
Metasurfaces are thin, artificially structured arrays of meta-atoms that allow manipulation of optical fields on a subwavelength scale. In this work, we show the emergence of chaotic-like behavior in a simplified model of a metasurface with spatiotemporal dynamics. The system is modeled on three levels. First, the incident light is described using a random walk model to introduce temporal phase fluctuations. Second, the metasurface is treated as an anisotropic structure that introduces spatially varying amplitude and phase shifts. Finally, the resulting field is propagated using Fresnel diffraction to obtain the output intensity. We demonstrate that this simple model exhibits signatures of chaotic-like dynamics, including the formation of attractors and characteristic relationships between frequency components and the power spectral density. These results highlight how complex behavior can emerge from simple optical systems.

Keywords: Metasurfaces; Random walk; Chaos

1. Introduction

1.1. Metasurfaces

Metasurfaces are artificially engineered two-dimensional structures composed of arrays of meta-atoms, which are subwavelength scatterers. They enable local control of electromagnetic waves, enabling manipulation of phase, amplitude, and polarization on subwavelength scales. This makes it possible to shape optical wavefronts in ways not achievable with conventional optics (Hu et al., 2021).

1.2. Classification of Metasurfaces

Metasurfaces can be classified based on their response and time dependence (**Figure 1**) (Xu et al., 2021). Passive metasurfaces have a fixed response determined by their geometry and do not require external energy, while dynamic metasurfaces can change their response in time but require external control. We can also distinguish whether the incident light is time-dependent or time-independent. In this work, we focus on a passive metasurface with time-dependent input, leading to spatiotemporal dynamics in the output.

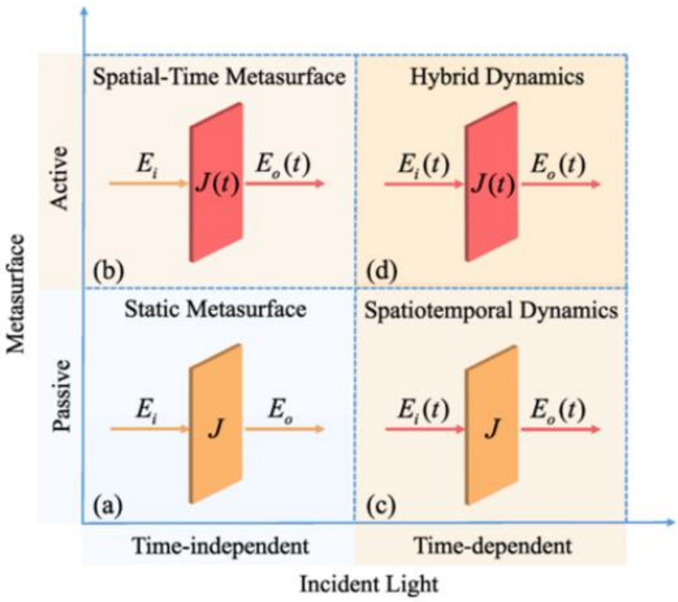

Figure 1. Classification of Metasurfaces (Xu et al., 2021). We can classify metasurfaces by whether they are passive or active in design (y-axis) and whether the incident light is time-dependent or independent (x-axis). The bottom row displays the passive metasurfaces, whose response is determined by geometry and cannot be changed. The top row shows the active metasurfaces whose configuration can be changed dynamically, but it needs an external source of energy. In the first column, the incident light is time-independent, and in the second column, the incident electromagnetic waves are time-dependent. The main focus of this work is the spatiotemporal dynamic metasurfaces that are passive, but the incident light is time-dependent.

2. Modeling

2.1. Incident light

We model the incident light $\boldsymbol{E}_{\text{in}}$ as having a time-dependent polarization angle $\theta(t)$:

$$\boldsymbol{E}_{\text{in}}(t) = (\cos\theta, \sin\theta), \tag{1}$$

which evolves as a random walk:

$$\theta(t + \mathrm{d}t) = \theta(t) + \sqrt{2D\mathrm{d}t}\xi(t), \tag{2}$$

where D is a diffusion coefficient, $\mathrm{d}t$ time step, and ξ Gaussian white noise (Romanczuk et al., 2012). At each time step t, the new angle at $t + \mathrm{d}t$ is given by its previous value plus a random increment, controlled by a diffusion coefficient D. If D is large, the signal becomes noisier; if it is small, the evolution is smoother. The variance of the fluctuations grows proportionally to $2D\,\mathrm{d}t$. In **Figure 2**, we see how the polarization angle evolves over time, and in **Figure 3**, how this determines the electric field components ($E_x = \cos\theta(t)$) and ($E_y = \sin\theta(t)$), and their evolvment over time. Since the input is stochastic, each realization is different.

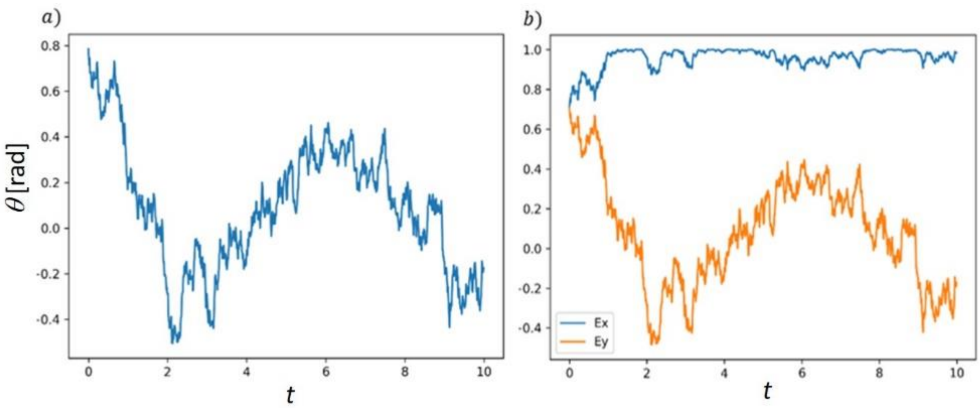

Figure 2. a): Evolution of the angle of the polarization ($\theta(t)$) with time step t. b) Evolution of electric field components (E_x blue line and E_y orange line)

2.2. Anisotropic metasurface

We model the metasurface as an optical element that transforms incoming light as follows:

$$\boldsymbol{E}_{\mathbf{out}} = J(\boldsymbol{r})\boldsymbol{E}_{\mathbf{in}} \,, \tag{3}$$

where we use a position-dependent Jones matrix J (Rubin et al., 2025),

$$J = \begin{pmatrix} J_{11}(x_1, y_1) & J_{12}(x_1, y_1) \\ J_{21}(x_1, y_1) & J_{22}(x_1, y_1) \end{pmatrix} \,, \tag{4}$$

with $\boldsymbol{r} = (x_1,y_1)$.

Each meta-atom introduces a local transformation that modifies the amplitude and phase of the electric field (**Figure 3**). The diagonal elements affect each component of polarization independently, while the off-diagonal elements introduce coupling between components, leading to cross-polarization. This polarization mixing is essential for generating complex behavior in the system. Therefore, each meta-atom introduces a different phase shift, resulting in a spatially varying wavefront, and this spatial disorder plays an important role in creating complex interference patterns.

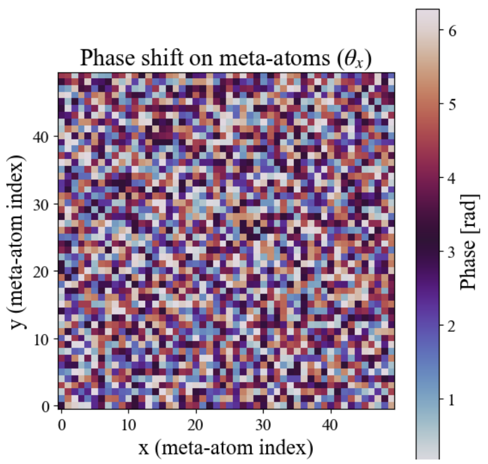

Figure 3. Phase shift on meta-atoms for x - component of angle θ (θ_x). x and y are the positions on the modelled metasurface. The colour represents the phase shift on each pixel, which corresponds to a meta-atom. Phase changes from 0 to 2π randomly for each meta-atom.

2.4. Intensity calculations

We analyze the light intensity I, which is proportional to the squared magnitude of the electric field $\boldsymbol{E}$:

$$I \propto |\boldsymbol{E}|^2 \ . \quad (5)$$

First, the intensity is calculated directly at the metasurface. The field $\boldsymbol{E_f}$ at distance z from the metasurface is then evaluated using the Fresnel diffraction integral (Born, 1999):

$$\boldsymbol{E_f}(x,y) = \frac{\mathrm{e}^{ikz}}{i\lambda z} \iint \boldsymbol{E}(x',y') \mathrm{e}^{\frac{ik}{2z}(x-x')^2+(y-y')^2} \mathrm{d}x' \mathrm{d}y', \quad (6)$$

where λ is the wavelength of the incident light, (x',y') represent coordinates at the metasurface plane, and (x,y) coordinates represent position at a distance z from the metasurface. Since the observation screen is located in the near field, we use Fresnel diffraction, which describes the propagaing in this regime. Light from different points on the metasurface acquires different phases during propagation and interference between them.

3. Results

3.1. Intensity directly after the metasurface

First we calculate the intensity directly at the metasurface. Using a diagonal Jones matrix (Eq. (4)), where off-diagonal elements are set to zero, there is no polarization mixing (**Figure 4a**), and the light intensity remains uniform. When off-diagonal terms are included (Eq. (4)) (**Figure 4b**), polarization components mix, leading to spatially varying intensity patterns. This shows that polarization coupling introduces spatial complexity.

3.2. Intensity distance $\boldsymbol{z}$ *after propagation*

Next, we calculate the light intensity after propagation. In both cases, interference leads to spatial variations. Even when the light intensity is uniform at the metasurface (**Figure 4a**), propagation introduces interference (**Figure 5a**). When polarization mixing is included, the patterns become even more complex (**Figure 5b**). Each pixel corresponds to a meta-atom, and we can see how the pattern continuously changes.

3.3. Temporal dynamics

We analyze the temporal behavior of the output intensity. Firstly, we plot the intensity at one time step versus the next, giving a phase-space representation of the dynamics (**Figure 6a**). We observe strong correlations between consecutive steps, resulting in an attractor-like structure. In the **Figure 6b**, we show the power spectral density. This is obtained by taking the Fourier transform of the intensity signal and computing the squared magnitude, which gives the power at each frequency. In log-log scale, the spectrum shows an approximately linear decay, indicating broadband frequency content and complex temporal behavior.

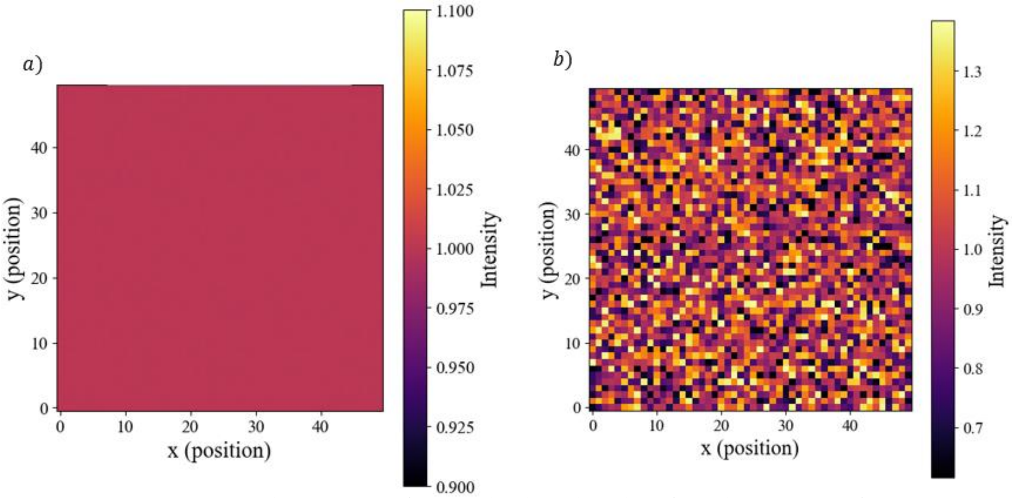

Figure 4. Intensity on the metasurface, calculated right after the metasurface. x-axis and y- axis represent the position at the metasurface. Each pixel is a modelled meta-atom on the metasurface. The intensity is represented with the color bar. a) The intensity of the each metaatom right after the metasurface, where the phase shift on the metasurface is modelled with diagonal Jones Matrix. b) Phase shift is modelled with full Jones matrix, allowing coupling between the components.

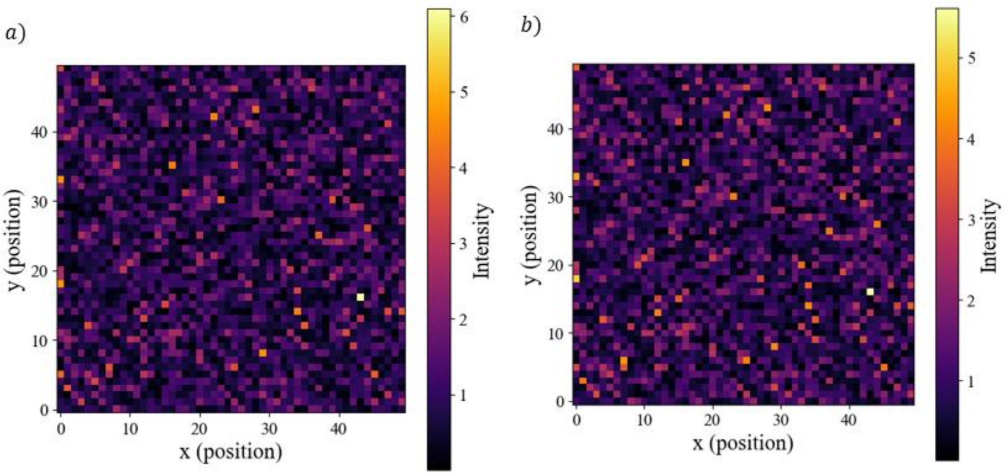

Figure 5. Intensity on the metasurface, calculated at distance z after the metasurface with Fr diffraction. x- and y- axis represent the position the metasurface. Each pixes is a modelled metaatom on the metasurfaces. The intensity is represented with the color bar. a) The intensity of the each metaatom at distance z after the metasurface, where the phase shift on the metasurface is modelled with diagonal Jones Matrix. b) Phase shift is modelled with full Jones matrix, allowing coupling between the components.

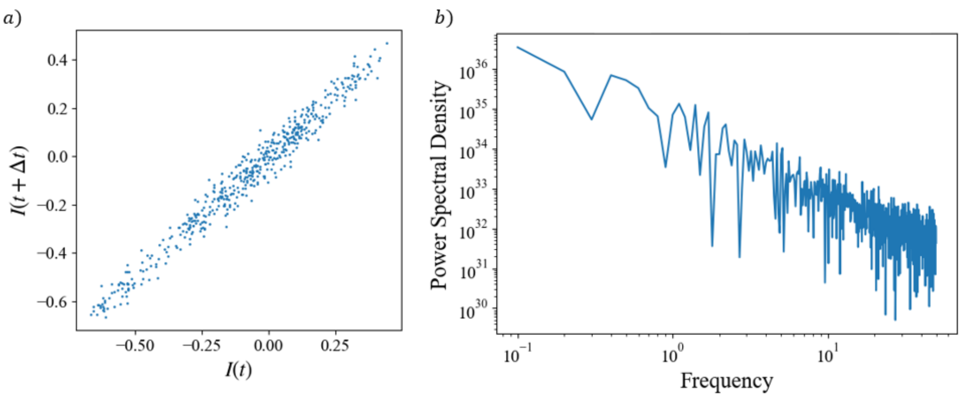

Figure 6. a) Intensity plotted at time step t on the x- axis vs the next time step $(t + \Delta t)$ on the y-axis, resulting in a chaotic like structure. b) Power sprectral density (PSD) of the Intensity plotted at each frequency (x- axis), calculated by firstly taking the Fourier transform of the Intensity at time t, and calculating power at each frequency.

3.4. Poincare spheres

Polarization can be represented using the Poincare sphere (**Figure 7**). The polarization state is described using the Stokes parameters and corresponds to a point on the sphere. Linear polarization lies on the equator, circular polarization at the poles, and elliptical polarization elsewhere (ScienceDirect Topics, 2026). The input remains mostly linear (**Figure 7a**), while the output explores a broader region, indicating more complex polarization states (**Figure 7b**).

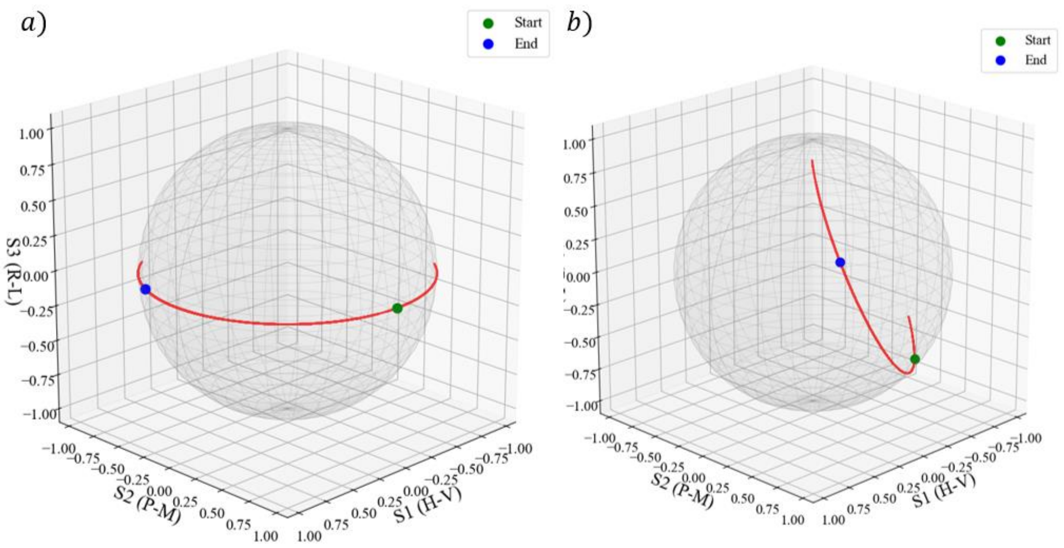

Figure 7. Poincare sphere representing polarization of the a) input field and the b) output field. On the x-axis is $S1$ Stokes parameter, on the y-axis is $S2$ Stokes parameter and on the the z-axis is $S3$ Stokes parameter. Input field is linearly polarized and output field is ellipticaly polarized.

4. Conclusions

In this work, we have shown that a simple model combining stochastic input, spatial phase modulation, and propagation can produce rich and complex behavior. The interplay between polarization mixing and interference leads to structured, dynamic output patterns. This demonstrates how metasurfaces can act as simple platforms for generating complex, chaotic-like optical dynamics.

Conflicts of Interest: The authors declare no conflict of interest.

References

1. Born M, Wolf E. Principles of Optics. 7th ed. Cambridge: Cambridge University Press; 1999.
2. Hu J, Bandyopadhyay S, Liu Y, Shao L. A Review on Metasurface: From Principle to Smart Metadevices. Front Phys. 2021; 8:586087. DOI:10.3389/fphy.2020.586087
3. Spectral density. Wikipedia. Available at: https://en.wikipedia.org/wiki/Spectral_density. Accessed April 28, 2026.
4. ScienceDirect Topics. Available at: https://www.sciencedirect.com/topics/physics-and-astronomy/poincare-spheres. Accessed April 28, 2026.
5. Romanczuk P, Bär M, Ebeling W, Lindner B, Schimansky-Geier L. Active Brownian particles. Eur Phys J Spec Top. 2012; 202:1–162. DOI:10.1140/epjst/e2012-01529-y
6. Rubin NA, Fainman Y. Polarization-sensitive diffractive optics and metasurfaces: Past is Prologue. Nanophotonics. 2025; 14:3825–3834. DOI:10.1515/nanoph-2024-0740
7. Xu M, Zhang F, Pu M, Li X, Ma X, Guo Y, Zhang R, Hong M, Luo X. Metasurface spatiotemporal dynamics and asymmetric photonic spin–orbit interactions mediated vector-polarization optical chaos. Phys Rev Res. 2021; 3:013215. DOI: 10.1103/PhysRevResearch.3.013215.